ELSEVIER

Low-threshold blue lasing in epitaxially grown para-sexiphenyl nanofibers

F. Quochi[a],*, A. Andreev[b], F. Cordella[a], R. Orrù[a], A. Mura[a], G. Bongiovanni[a], H. Hoppe[c], H. Sitter[b], N.S. Sariciftci[c]

[a]Dipartimento di Fisica, Università di Cagliari, I-09042 Monserrato (CA), Italy
[b]Institute for Semiconductor and Solid State Physics, Johannes Kepler University Linz, A-4040 Linz, Austria
[c]Linz Institute for Organic Solar Cells (LIOS), Physical Chemistry, Johannes Kepler University Linz, A-4040, Linz, Austria

Abstract

Random laser action and amplified spontaneous emission are observed near 425 nm in self-assembled para-sexiphenyl nanofibers following subpicosecond optical pumping. The threshold excitation fluence (photoexcited density) is as low as $0.5\,\mu J/cm^2$ ($6 \times 10^{16}\,cm^{-3}$). The high degree of material crystallinity results in a very large singlet–singlet annihilation rate of $\approx 10^{-7}\,cm^3/s$. In stationary conditions, assuming a standard singlet-to-triplet density ratio of 0.3 and bimolecular recombination as the only density-dependent loss mechanism, the equivalent current density necessary for lasing threshold is estimated to be as low as $3\,kA/cm^2$. The experimental findings suggest that such highly ordered molecular nanoaggregates have great potential as blue-emitting devices for integrated photonic applications.
© 2004 Elsevier B.V. All rights reserved.

Recent advancements in the field of epitaxial growth include surface-dipole-assisted self-assembly of nanoaggregates of organic molecules, such as para-sexiphenyl (p-6P). Crystalline needle-shaped [1,2] and ring-shaped [3] aggregates of p-

6P have been realized on both mica and KCl substrates; the nanoaggregates are truly nanoscopic in two dimensions (their heights and widths), while their lengths and radii are in the millimeter- and micrometer-length scale. The size and surface density of the needles can be controlled through the growth parameters and by laser irradiation [4]. Due to the high blue luminescence quantum yield (30%) of p-6P in the

*Corresponding author. Tel.: +39 070 6754843;
fax: +39 070 510171.

E-mail address: francesco.quochi@dsf.unica.it (F. Quochi).

solid state and to their crystalline structure, p-6P nanoaggregates are easily envisaged as highly polarized, blue-emitting basic components (such as active waveguides and resonators) of next-generation integrated photonic systems. Linear waveguiding of the p-6P blue emission near 425 nm has been demonstrated in the needles (nanofibers) [5]. Nonlinear optical conversion (second-harmonic generation and two-photon luminescence) has also been reported, in both the nanofibers and nanorings [3,6]. Owing to the waveguiding effect, amplified spontaneous emission (ASE) and lasing are also possible in these nanoaggregates. However, no clear signature of ASE or lasing emission had ever been reported in either the nanofibers or nanorings until very recently [7].

In this paper, we report experimental evidence of amplified spontaneous emission and random lasing near 425 nm in p-6P nanofibers grown by hot-wall epitaxy (HWE) on freshly cleaved, (0 0 1)-oriented mica substrates. Evaporation of p-6P is operated under a dynamic vacuum of $\approx 10^{-6}$ mbar, at a substrate temperature ranging typically from 80 to 130 °C. Self-assembly of the p-6P molecules results in needle-shaped nanofibers, featuring cross-sectional dimensions in the 100-400 nm range (depending upon growth conditions), and lengths of up to 100 μm. The high order of crystallinity of p-6P has been shown to yield highly polarized optical absorption [2,8].

ASE and laser action are investigated by photopumping with ultra short pulses. Photoexcitation is performed using the frequency-doubled output pulses (760 nm, 150 fs duration) of a Ti:sapphire regenerative amplifier operating at the repetition frequency of 1 kHz. The 380-nm excitation beam is focused to a spot size of 120 μm, approximately, so that even the longest nanofibers can be thoroughly excited upon suitable positioning of the laser spot on the sample surface. The excitation polarization is set parallel to the long molecular axis for maximum material absorption ($A \approx 60\%$). The samples are placed inside a recirculating-loop cold-finger cryostat and optical measurements are performed over the 30–300 K temperature range. The emission is collected by variable numerical aperture optics and dispersed in a single spectrometer. A LN_2-cooled charge-coupled device is used to measure the time-integrated emission spectra.

The experiments and related results reported in this paper refer to a nanofiber sample grown at a substrate temperature of 130 °C, whose surface topography image, obtained by an atomic-force microscope (AFM) in tapping mode, is shown in Fig. 1.

From a line profile reconstructed along the direction perpendicular to the needle axis we deduce an average base width and height of the nanofibers of about 220 and 110 nm, respectively. The nanofibers result to be highly packed, having a surface coverage factor of $\approx 50\%$. Since (i) it was shown that the nanofibers can support light propagation at 425 nm if their width is larger than 220 nm [5], and (ii) in virtue of the very little amount of p-6P material present between adjacent needles [2], we infer that ASE and laser action at the 0–1 vibronic peak (425 nm) are possible only along the fibers lying in the upper side of the fiber width distribution.

Fig. 2 shows room-temperature emission spectra collected normally to the sample surface with an f-number (f/#) of ≈ 4, for different values of the excitation fluence. Owing to strong light scattering by the nanostructured surface of the sample, the emission is rather isotropic; the emission spectra measured using collecting optics with different
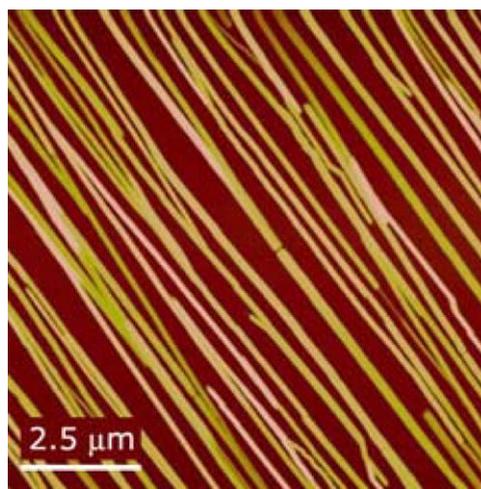

Fig. 1. AFM topography image of the surface morphology of a p-6P film grown by HWE at 130 °C on (0 0 1)-oriented mica.
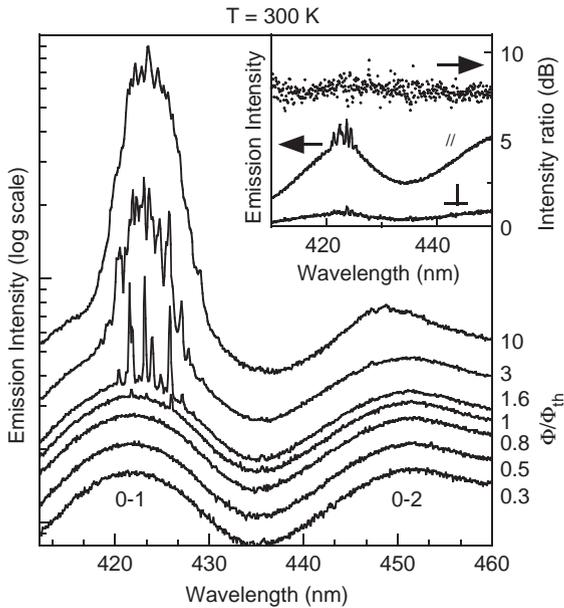
Fig. 2. Main panel: Room-temperature, time-integrated emission spectra for different values of the pump fluence Φ/Φ_{th}, where $\Phi_{th} \approx 1\,\mu J/cm^2$ per pulse. Inset: Emission spectra measured after polarization filtering along the direction parallel (//) and perpendicular ($\perp$) to the long molecular axis of p-6P (solid lines); Intensity ratio between the two polarization filtered spectra (dots).

numerical apertures, at various angles, display very similar features.

When the excitation fluence reaches threshold values (Φ_{th}) of $1\,\mu J/cm^2$ (per pulse) or lower, ultra narrow (width $< 2\,\text{Å}$) and randomly spaced lines suddenly appear on top of the spontaneous emission spectrum near 425 nm. The threshold fluence is found to be independent of temperature down to 30 K, and position dependent with typical variations of a factor of 3. Assuming that the conversion efficiency of the absorbed pump energy into singlet excitons is equal to 100%, the (lowest ever observed) threshold fluence $\Phi_{th} = 0.5\,\mu J/cm^2$ yields a threshold density (N_{th}) of $6 \times 10^{16}\ cm^{-3}$. The optical emission is highly polarized, with an output polarization intensity ratio larger than 7 dB (inset of Fig. 2).

Since the spectral pattern is (i) strongly dependent on the photoexcited area on the sample, and (ii) time independent, so that detection artifacts can be completely ruled out, the narrow lines are

attributed to random laser action occurring along the nanofibers. The optical feedback necessary for laser action originates presumably from random fiber width fluctuations. Random laser action has been reported over the last few years in a variety of solid-state, high-gain material systems [9], including neat films of substituted thiophene-based oligomers, which possess very large stimulated-emission cross-sections of up to $6 \times 10^{-16}\,cm^2$ at the material gain peak [10].

As the excitation fluence is increased, an ASE band appears on top of the 0–1 vibronic band, which explains the superlinear variation of the nonlinear emission intensity with pump excess fluence, $(\Phi - \Phi_{th})/\Phi_{th}$ [7]. Also, we have partial evidence of ASE threshold at the peak of the 0–2 vibronic band near 450 nm at the highest excitation fluence of $\Phi/\Phi_{th} \approx 10$ (Fig. 2). Random lasing starts in a few nanofibers exhibiting long closed-loop random paths for light amplification, which causes the appearance of narrow spikes on top of the broad spontaneous emission spectrum of the photoexcited nanofibers. At sufficiently high pump fluences, ASE takes place even in the lossier nanofibers (not possessing efficient random gain paths) and line narrowing of the 0–1 vibronic band is then observed.

Density-dependent effects are observed in spectrally- and time-integrated measurements of the spontaneous emission intensity as a function of the excitation fluence, for pump fluences below lasing threshold (Fig. 3 (a)). The sublinear behavior indicates the occurrence of density-dependent losses, which are attributed to singlet–singlet annihilation [11]. The time-integrated emission intensity is curve fitted using the function $I(N_0) \propto \ln(k_{SS}N_0/k_0 + 1)$, where k_{SS} and k_0 are the singlet-singlet annihilation coefficient and the (low-intensity) inverse photoluminescence lifetime, respectively, and N_0 is the estimated singlet density at the time of excitation ($t = 0$). Using $k_0 = 1.8 \times 10^9\ s^{-1}$ [7], we find $k_{SS} = (0.9 \pm 0.2) \times 10^{-7}\ cm^3/s$. We conclude that the bimolecular (nonradiative) recombination coefficient is as large as $10^{-7}\ cm^3/s$, which is in fact comparable to the value reported in tetracene single crystals [12]. The efficient singlet–singlet annihilation process is attributed to the high molecular order of the p-6P nanofibers,
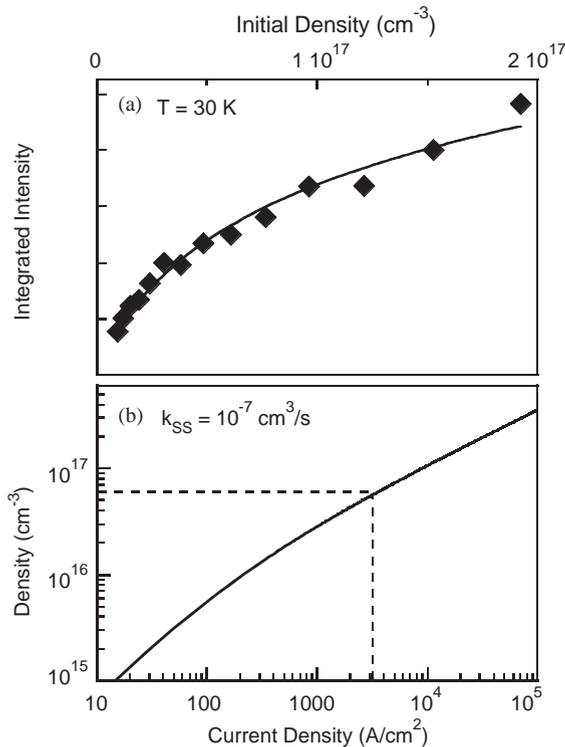
Fig. 3. (a) Spectrally and time-integrated emission intensity versus photoexcited singlet density N_0 at $t = 0$, for pump intensities below threshold ($T = 30\,K$). The solid diamonds are the experimental points and the solid line is a fit to the data (see the text for details). (b) Steady-state singlet density as a function of the current density, calculated as explained in the text. The horizontal and vertical dashed lines mark the threshold density $N_{th} = 6 \times 10^{16}\,cm^{-3}$ and the corresponding threshold current density $J_{th} = 3\,kA/cm^2$, respectively.

which would result in a large diffusion constant of singlet excitons.

Given $k_{SS} = 10^{-7}\,cm^3/s$, bimolecular recombination dominates the singlet recombination dynamics for densities larger than $N_{SS} = 2 \times 10^{16}\,cm^{-3}$. The current density necessary to achieve a given singlet density in a DC electrical pumping scheme is estimated with the assumption that only singlet–singlet annihilation is responsible for density-dependent losses. In fact, it is known that singlet–polaron interaction is weaker than singlet–singlet interaction in crystalline materials

[11]. A standard value of 0.3 is taken for the singlet-to-triplet population density ratio at the steady state. The thickness of the recombination region is set equal to the average thickness of the nanofibers (110 nm). The variation of the singlet density with current density is shown in Fig. 3 (b). We notice that a threshold density $N_{th} = 6 \times 10^{16}\,cm^{-3}$ yields an equivalent threshold current density $J_{th} = 3\,kA/cm^2$, which might be achievable in high-mobility crystalline materials [11]. This suggests that electrical pumping is potentially feasible in crystalline *p*-6P nanofibers.

In conclusion, we report evidence of low-threshold random laser action and ASE near 425 nm in *p*-6P self-assembled nanofibers grown by HWE. The high molecular order of the nanofiber material makes them attractive as highly polarized, blue-emitting nanoscaled devices for integrated photonics applications in the near future.

References

[1] F. Balzer, H.-G. Rubahn, Appl. Phys. Lett. 79 (2001) 3860.
[2] A. Andreev, G. Matt, C.J. Brabec, H. Sitter, D. Badt, H. Seyringer, N.S. Sariciftci, Adv. Mater. 12 (2000) 629.
[3] F. Balzer, J. Beermann, S.I. Bozhevolnyi, A.C. Simonsen, H.-G. Rubahn, Nano Letters 3 (2003) 1311.
[4] F. Balzer, H.-G. Rubahn, Nano Letters 2 (2002) 747.
[5] F. Balzer, V.G. Bordo, A.C. Simonsen, H.-G. Rubahn, Phys. Rev. B 67 (2003) 115408.
[6] F. Balzer, K. Al Shamery, R. Neuendorf, H.-G. Rubahn, Chem. Phys. Lett. 368 (2003) 307.
[7] F. Quochi, F. Cordella, R. Orrù, J.E. Communal, P. Verzeroli, A. Mura, G. Bongiovanni, A. Andreev, H. Sitter, N.S. Sariciftci, Appl. Phys. Lett. 84 (2004) 4454.
[8] H. Plank, R. Resel, H. Sitter, A. Andreev, N.S. Sariciftci, G. Hlawacek, C. Teichert, A. Thierry, B. Lotz, Thin Solid Films 443 (2003) 108.
[9] H. Cao, Y.G. Zhao, S.T. Ho, E.W. Seelig, Q.H. Wang, R.P.H. Chang, Phys. Rev. Lett. 82 (1999) 2278.
[10] D. Pisignano, M. Anni, G. Gigli, R. Cingolani, M. Zavelani-Rossi, G. Lanzani, G. Barbarella, L. Favaretto, Appl. Phys. Lett. 81 (2002) 3534.
[11] M.A. Baldo, R.J. Holmes, S.R. Forrest, Phys. Rev. B 66 (2003) 035321.
[12] A.J. Campillo, R.C. Hyer, S.L. Shapiro, C.E. Swenberg, Chem. Phys. Lett. 48 (1977) 495.